Modeling the influence of rheology on smooth rod coating systems

JOHN A. ROPER III, DOUGLAS W. BOUSFIELD, AND GREGORY W. WELSCH

ABSTRACT: Rod coating methods are of interest for the application of barrier coatings, especially at off-line facilities that may run at moderate speeds and narrow web widths. At lower line speeds and lower coating solids, it is difficult to achieve good coat weight control because of poor loading of the rod. While there is extensive literature available about blade and roll coating, there seems to be less reported on the rod loading of smooth rods to obtain various coat weights. Much of the work is around metering rods working on applicator rolls at high speeds that are associated with the metered size press, with a focus on ribbing instabilities. This work employs a simplified model, neglecting some complex features of rubber deformation and film split, to estimate the influence of the process parameters such as speed, rod diameter, viscosity, and rod loading on the coat weight obtained. As found in practice, at low speed and low viscosities, the coat weight-load curve is steep, leading to poor control of the coat weight and coat weight uniformity. If the viscosity is increased, the curve is modified, and control is possible with rod loading in a normal range. For shear thinning fluids described by the Carreau model, the power law index and other parameters need to be in the correct range to obtain the desired effect. Modeling predictions show a steeper dependence of coat weight with rod pressure when compared to pilot coater data. This may be caused by missing details in the mechanical loading of the rod related to tube pressure or from neglecting the impact of filter cake formation of the applied coating in the model.

Application: The model and experimental results should help guide the smooth rod coating of paper grades, especially for barrier coatings applied off line.

Smooth rod coating is a well-established coating process for the paperboard industry and offers advantages over blade coating in providing a more uniform surface coverage. This feature makes rod coating an attractive option for applying barrier coatings, especially on off-line coaters or at packaging converting facilities. Over the years, the industry has developed a working knowledge for using rod coaters to apply highly pigmented coatings at medium-to-high line speeds. It is well known that rod applied coat weights have a lower response to rod pressure than blade coating. This necessitates the switch to different rod diameters and/or changing the coating solids to access a target coat weight range. However, the increasing use of smooth rod applied barrier coatings at relatively low line speeds and possibly lower solids creates the challenge of selecting the right rod diameter and tuning the rheology of the coating to achieve a high enough coat weight for good barrier performance. Because many barrier coatings are low in pigmentation and have Newtonian-like rheology, the coat weight response to rod pressure can deviate from the empirically known behavior of highly pigmented, shear-thinning paper coatings.

Despite the widespread use of rod coaters, there is little published work on the fundamentals of smooth rod coating. A limited amount of literature dates from the 1990s, and much of this work focuses on the use of a smooth rod to apply coatings to the transfer roll on metered size press (MSP) coaters. The MSP coaters can operate at much higher line speeds, so there were several issues, such as rod spitting and ribbing, that needed to be addressed. Some excellent experimental and sophisticated modeling work was done on the topic [1,2]. Another publication highlighted the importance of extensional viscosity for determining coat weights on a rod coater [3].

In contrast, blade coatings and roll coatings have been extensively studied both experimentally and theoretically. The models for these methods of application have grown increasingly complex and now incorporate features such as coating dewatering and deformation of backing rolls, as well as flexing of the blade under an applied load. Such a detailed understanding is lacking for rod coaters; for example, not knowing how a given rod diameter with a given coating rheology will respond to applied pressure, which is the subject of this investigation.

The motivation behind this work is to apply the well-established framework for modeling of roll and blade coatings [4-7] to smooth rod coatings to better understand the fundamentals of smooth rod coating. The strategy will be to start with a simple model to look at the effect of coating viscosity, rod diameter, and coating speed on coat weight for both Newtonian and shear-thinning coating, while ig-

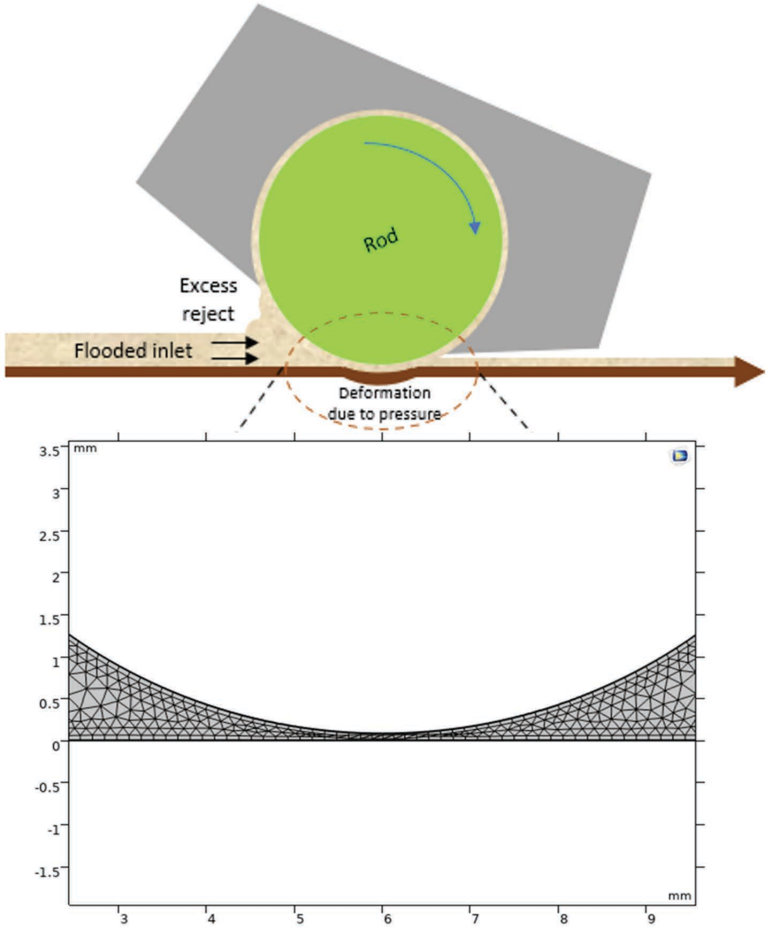

1. Side view of rod coating with excess coating supplied upstream and film split downstream. The rod often rotates slowly. The region of interest is zoomed, and the finite element mesh is shown.

noring features like compressibility, film split, dewatering, and wall slip. These simulations are compared to published experimental results. The work presented here is a first step in developing robust models for rod coatings.

MODEL DEVELOPMENT

The flow between a metering rod and a substrate is known to follow lubrication analysis well. The complexity comes from the exit region of the rod and the film split that occurs there. In that region, some of the coating will stay with the rod and the rest will move with the web. **Figure 1** shows the situation of interest. The amount of fluid that stays with the rod is likely small if the rotational speed of the rod is low. The film split location is controlled by a balance of viscous and surface tension forces.

Because of the interest in studying shear thinning fluids and other complex viscosities, a commercial finite element code is used (COMSOL Multiphysics Version 5.4, COMSOL AB; Stockholm, Sweden). The bottom part of Fig. 1 shows the mesh that is used for physics-controlled meshing. The geometry is generated by subtracting a circle equal to the rod diameter from a rectangle of the region of interest. The circle position is the gap between the rod and the web plus the rod radius. The laminar flow physics is selected and either Newtonian or non-Newtonian rheology is selected. This causes the program to solve the normal conservation of mass and momentum equations. The boundary conditions are the web velocity at the lower boundary, the rod velocity at the top boundary, and a zero-gauge pressure condition for the inlet and outlet regions. The influence of the film split is neglected here because of the focus on rod loading; most of the pressure generation is in the region in the center of the nip. In addition, rubber or web deflection is neglected. A typical pressure distribution is shown in **Fig. 2**. Pressure builds in front of the rod but then rapidly falls to subambient values right after the minimum gap. This agrees with other reported predictions, although a number of factors are neglected here, as shown in **Table I**.

Most experimental measurements of the pressure distribution do not show a pronounced subambient pressure, as in Fig. 2. This may be caused by the short duration of the pulse, cavitation phenomena, film split invading the region, or the relaxation of rubber deformation. In view of the com-

Assumptions	Potential Impact on Modeling Results
Flat nonporous substrate with no filtercake formation	Earlier modeling work with metered size press (MSP) coatings showed that filter cake formation was a key factor in coat weight control.
Rheology unchanged due to dewatering	Past work modelling blade coating suggests filter cake formation is more important than viscosity change.
No extensional viscosity effects	Extensional viscosity will increase the pressure needed to achieve a target coat weight, but overall trends should be similar [3].
No deformation of substrate or backing roll	Past modeling of roll coatings suggests impact on film split and ribbing instabilities, as well as negative pressure pulse at the exit. There is an uncertain impact on coat weight response.
No cavitation or film split at the exit of the rod nip and not including this in the loading calculation	While coating that makes it through the minimum gap will end up on the web, the load predictions may be influenced by this. Experimental pressure measurements show only a small subambient pressure, possibly due to cavitation.
Rod is not rotating and no water lubrication layer on the rod	Rod rotation speed is small compared to web velocity. Rod rotation is known to impact rod spitting and streaking. Lubrication may help coating to slip under rod as plug flow, increasing coat weight and lowering effective shear rate.

I. List of model assumptions.

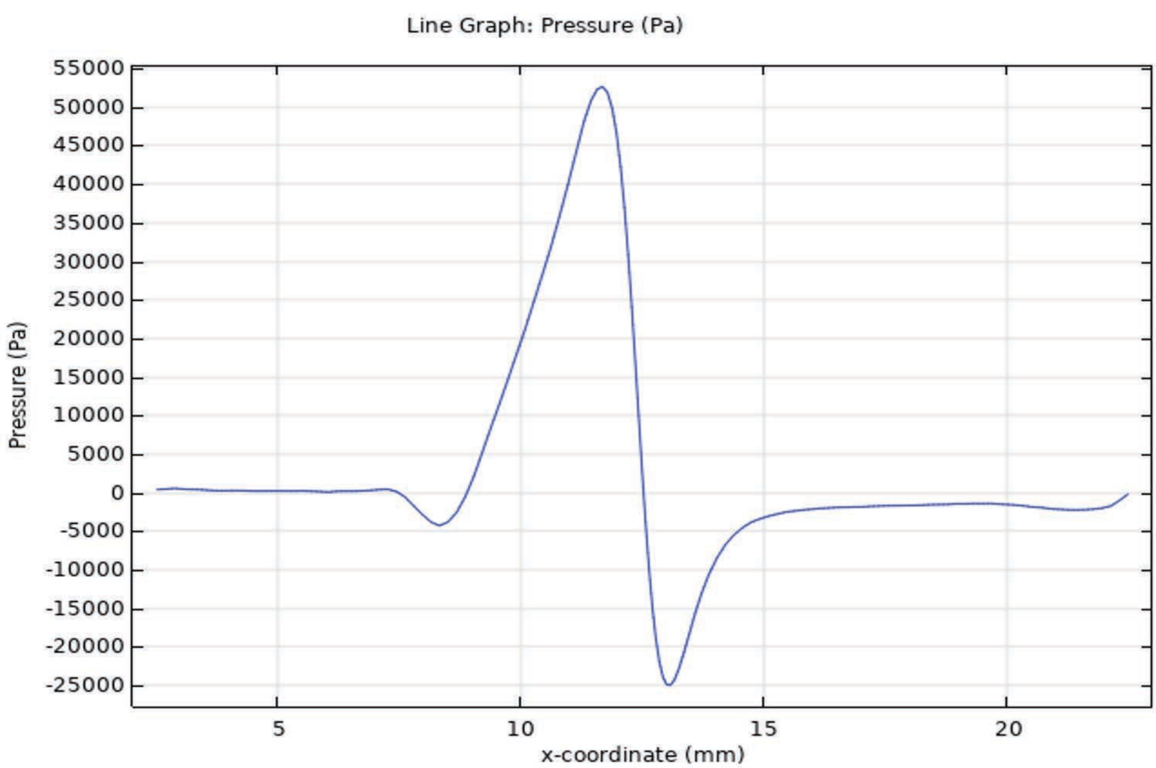

2. Pressure predictions for rod diameter of 25 mm, velocity of 10 m/s, viscosity of 10 mPas, and a rod-web gap of 50 mm.

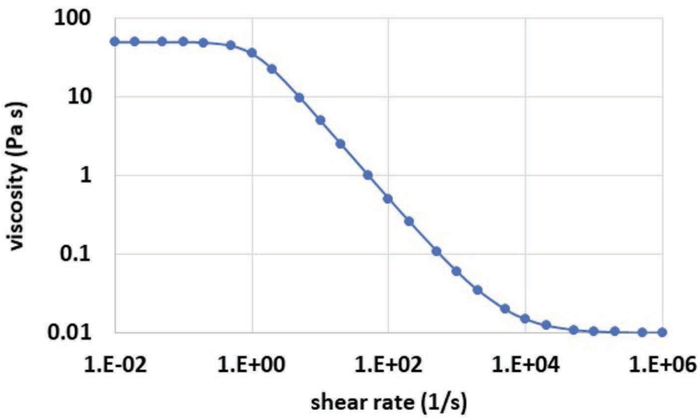

3. Typical shear thinning behavior described by Carreau model.

plexity and uncertainty of this region, the pressure distribution is not certain. Therefore, to determine the rod loading, only the pressure distribution in front of the minimum gap is integrated to obtain the estimated rod loading. The coat weight or coating thickness is determined by integrating the velocity profile at the exit of the region, which should match the net flow anywhere along the region to conserve mass.

To investigate the influence of rubber deformation on the behavior of the rod coater, the lubrication approximation for fluid flow in a thin gap is used. This assumes incompressible Newtonian flow and that the gap between the rod and the paper is small compared to the rod diameter. The lubrication equation is:

$$\frac{dP}{dx} = \frac{12\mu}{h^3}\left(\frac{Uh}{2} - Q\right) \quad (1)$$

where h is the distance from the rod to the paper, U is the web speed, m is viscosity, and Q is the flow rate through the nip per unit width. The pressure P increases as fluid is pulled into the gap and then decreases as it moves out of the rod-paper gap. Taking into account the rubber deformation can be done by allowing the gap to be a linear function of the local pressure [8]. A simple equation is:

$$h = ho + P/K_E \quad (2)$$

where ho is the gap for no rubber deformation, and K_E is some constant that should depend on the hardness of the rubber or the elastic modulus of the rubber backing. This equation changes the geometry of the rod-paper gap as a function of the local pressure.

The lubrication equation is integrated numerically with boundary condition of no pressure at inlet and exit of the region, adjusting Q to obtain the exit pressure condition.

When thickeners are added to coatings, often a shear thinning rheology is obtained. One convenient method to capture a broad range of shear rates typical of these fluids is the Carreau model, given as:

$$\mu = \mu_\infty + (\mu_o - \mu_\infty)(1 + (\lambda\gamma)^2)^{(n-1)/2} \quad (3)$$

where μ_{oo} and μ_o are the high shear rate and low shear rate viscosity limits, λ is a time constant, and n is the power law index. **Figure 3** shows the viscosity function of a Carreau fluid.

In practice, the actual gap between the rod and the web is not known, but what is controlled is the rod loading by a pressure tube. The tube presses a rod support structure against the rod toward the web. When forces are balanced with the hydrodynamic lift, some gap will be obtained. To convert rod loading to the pressure tube applied, details of the support structure and how it interacts with the pressure tube and the rod are needed. Here, just the rod loading in N/m is reported, which represents the force per unit length of the rod, but when comparing with pilot data, the rod diameter is used to convert the force per width to a pressure. A force balance can also be used to link tube pressure to rod loading. The coat weight at that loading is then of interest.

Because of the number of parameters, dimensionless groups can be used to simplify the situation. Natural scaling parameters are the web velocity, rod diameter, and viscosity. A dimensionless rod loading F^* is obtained by dividing load F by viscosity and velocity. Others have suggested this scaling [2]. A Reynolds number is obtained from density, web velocity, rod diameter, and viscosity. A dimensionless coat weight can be obtained by dividing wet thickness by rod diameter. Here, the coat weight is reported for a dimensionless rod loading (F^*) and a Reynolds number (Re)

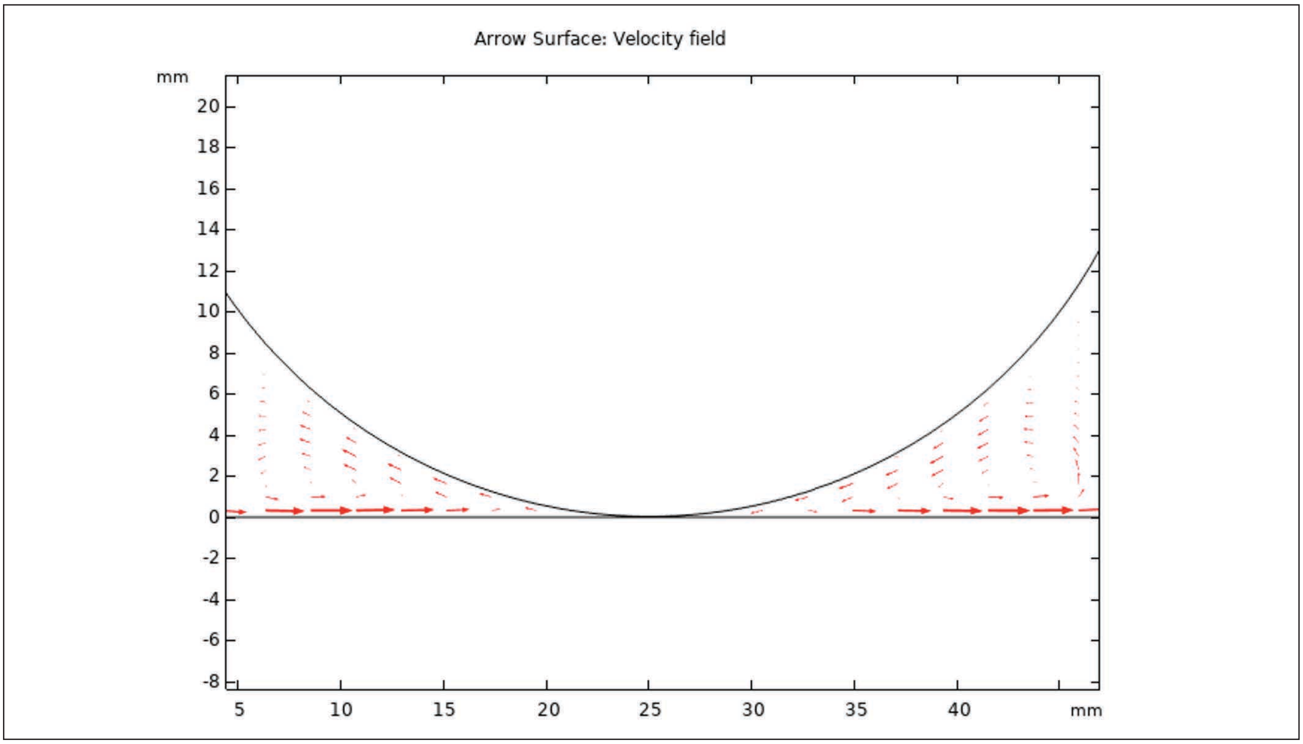

4. Velocity distributions for base case: left is for the inlet region, and right is for the exit region.

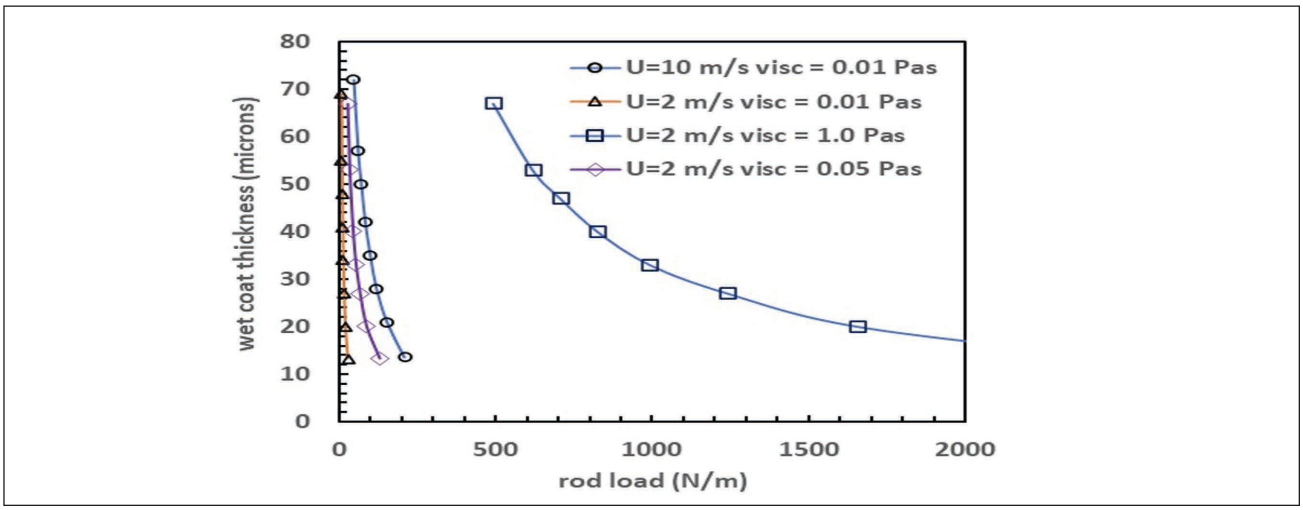

5. Results for a Newtonian fluid with viscosities of 0.01, 0.05, and 1.0 Pas at velocities of 2 and 10 m/s for a 25-mm rod.

defined as:

$$F^* = F/(U\mu) \tag{4}$$

$$Re = \rho UD/\mu \tag{5}$$

MODEL RESULTS

The velocity field and pressure distribution agree with what others have reported. **Figure 4** shows the velocity vectors in the inlet and outlet region of the rod. As expected, fluid is pulled into the nip by the web, but the small gap causes most of the fluid to be rejected and turned back. Figure 4 shows that most of the fluid that does get through the nip should tend to travel with the web. The circulation region shown on the outlet side likely does not exist because of the film split that would occur.

The influence of rod loading on expected coating wet thickness is shown in **Fig. 5** for a high-velocity case and two low-velocity cases. For velocity of 2 m/s and viscosity of 0.01 Pas, the curve is steep and near the y-axis, which indicates that a small change in the rod load leads to a large change in wet thickness. This condition would lead to difficulties in controlling the coat weight, and even along the rod, fluctuations in coat weight would be expected. The

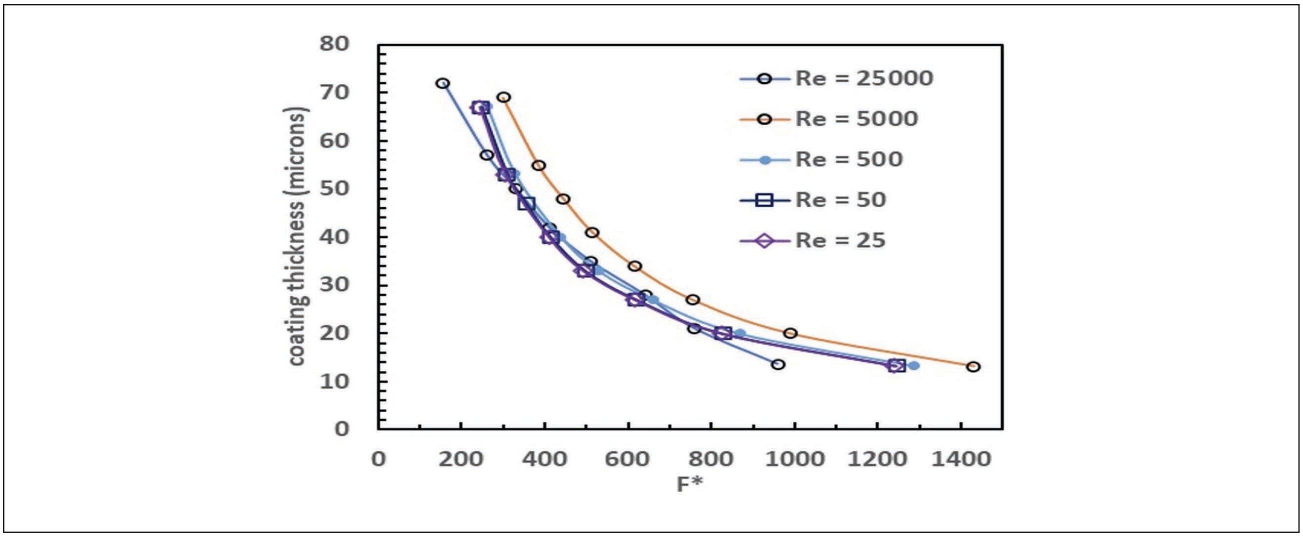

6. Wet coating thickness as a function of the dimensionless rod loading $F^* = F/U\mu$.

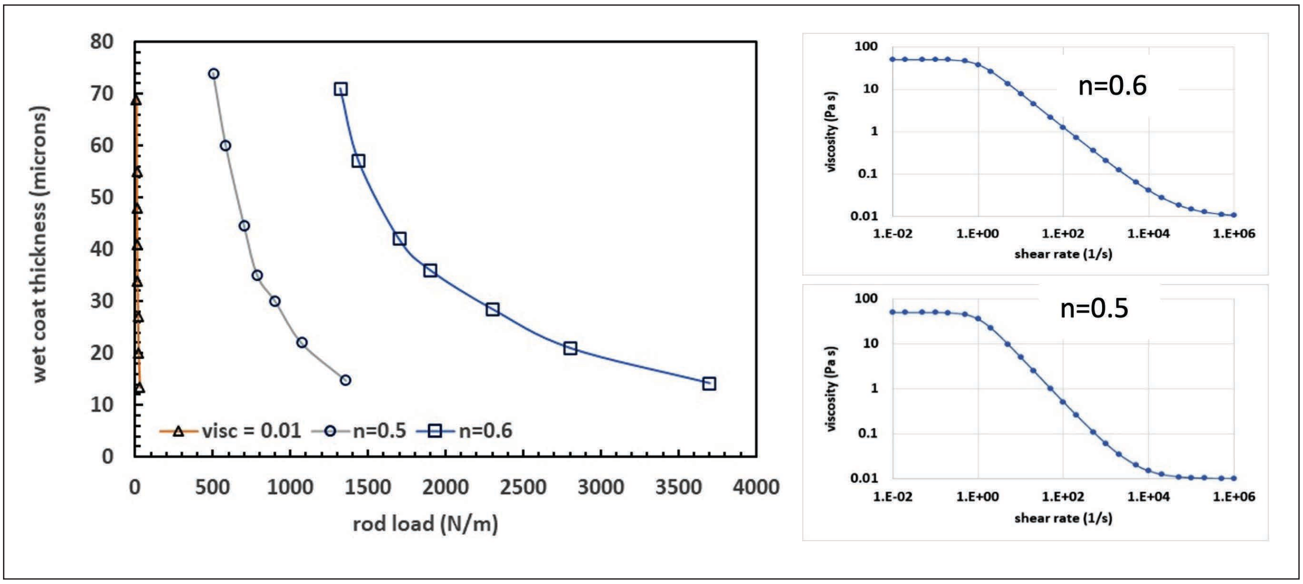

7. Rod loading for Carreau cases with λ *= 1 s;* h_{oo} *= 0.01 Pas;* h_o *= 100 Pas, and* n *= 0.5 and 0.6.*

conditions just do not generate much hydrodynamic lift on the rod to allow this to operate. For the high-speed low-viscosity case, the situation is better, but it could be a challenge depending on the pressure control and the uniformity of the situation. For the high-viscosity low-speed case, a range of rod loading gives a nice response to coat weight. This steep response is why wire-wound or grooved rods are of high value where the metering does not depend on rod loading via hydrodynamic forces.

Also of note is that the coating thickness is highly dependent upon the gap that is set and that the ratio of wet thickness to gap is in the range of 0.66 to 0.7; this result agrees well with the volume metering reported by Hanumanthu and Scriven [9].

For the Newtonian case, these different curves tend to collapse onto a single trend line when plotted as F^*. **Figure 6** shows the results for the cases in Fig. 5 plus another curve for a web velocity of 1 m/s. The conditions for different Reynolds numbers represent different web velocities. These are all for the same rod diameter of 25 mm.

For the Carreau model, when the high shear viscosity is set to 0.01 Pas, the model then predicts larger viscosities and hydrodynamic lift than the Newtonian case if the shear rates are not large in the nip region. **Figure 7** shows the results for the Newtonian case in Fig. 5, and the Carreau model with n = 0.5 and n = 0.6 and the zero shear viscosity of 100 Pas and λ = 1.0 s. The Carreau model cases push the loading results to a higher value of loading with a systematic change in thickness vs. load. This is because n = 0.5 and n = 0.6 cause the shear thinning to span over a large shear rate range. The shear rate at the minimum gap is ~40,000 1/s for the low wet thickness case. Multiple simu-

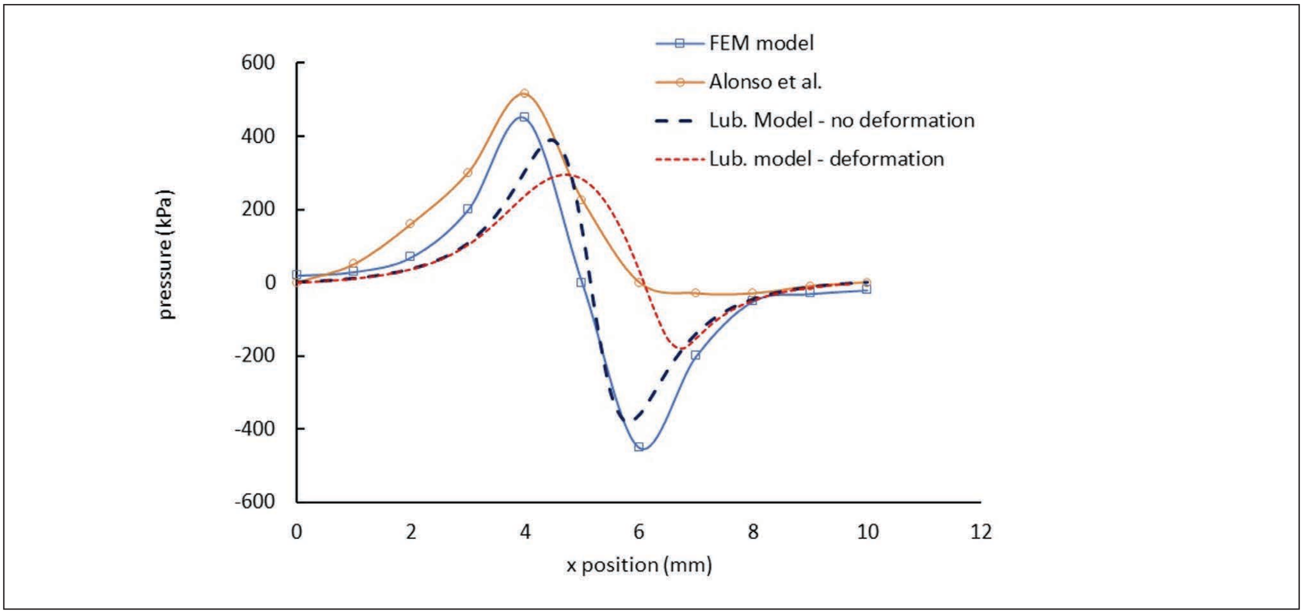

8. Measured pressure distribution by Alonso-Romero [10] compared to the finite element method (FEM) model and the lubrication model without deformation and the lubrication model accounting for deformation.

lations varying the Carreau model parameters suggest that the shear thinning behavior in this shear rate range is more important than the magnitude of the high shear viscosity in determining the coat weight vs. rod load response.

Comparison with pressure profile data

Accounting for deformation in the nip reduces the subambient pressure at the rod exit. The results are shown in **Fig. 8** for the same rod diameter, web speed, and gap using a Newtonian viscosity of 0.03 Pas as reported by Alonso-Romero [10]. While the exact parameters that account for the rubber hardness (deformation) are not known, as the parameter K_E is reduced, the shape of the pressure distribution does move closer to that reported in terms of a smaller subambient pressure. Without deformation, the lubrication model predicts a similar shape as the finite element model in that the positive and negative pressure values are symmetrical. The pressure is underpredicted because the lubrication equation does not take into account the non-Newtonian rheology. High deformation is hard to converge numerically, but the trend is clear in that the subambient pressure decreases as rubber deformation occurs. Therefore, using just the positive part of the pressure distribution to calculate load seems like a good approximation when neglecting the rubber deformation.

Comparison with pilot coater data

The predictions of our simplified model were compared to pilot coater data that was generated on the Trinseo pilot coater in Midland, MI, USA. This pilot coater study used coatings at three different solids levels, applied with rod diameters ranging from 9 mm to 19 mm using three different rod loading pressures [11]. The pilot coater data was analyzed using statistical software to develop predictive models. The analysis showed that solids level was a key parameter, but it appeared as a quadratic factor and as a cross term between solids and rod diameter, meaning there was no simple linear response. For example, when using the largest diameter rod at the highest solids, the coat weight was lower than that of using smaller diameter rods at the same rod pressure. Also, in some cases coat weight increased as rod pressure increased, similar to the response of a bent blade. This suggests that, much like blade coating, the geometry in the nip zone between the rod and substrate (which in turn depends on the degree of deformation of the backing roll) can lead to different classes of flow behavior. Understanding this aspect of rod coating is outside the scope of this modeling effort. Because of these complexities, a subset of the pilot coater data was selected to compare with modeling predictions. This subset of data showed the expected trends of increasing coat weight with rod diameter and decreasing coat weight with increasing pressure for all the rod diameters selected.

One of the challenges in using the pilot coater data is how to convert the measured applied pressure in an inflatable rubber tube located behind the rod bed assembly to the effective load on the rod in terms of force per unit width. As shown in **Fig. 9**, each rod diameter is mounted in its own rod holder that could transmit the tube pressure differently than one might expect from the change in rod diameter alone. In addition, the pressure applied to the rubber tube needs to deform the tube itself, which could change the dimensions in contact with the rod bed. An exact comparison could be done if a calibration is performed by applying pressure in the rubber tube and mea-

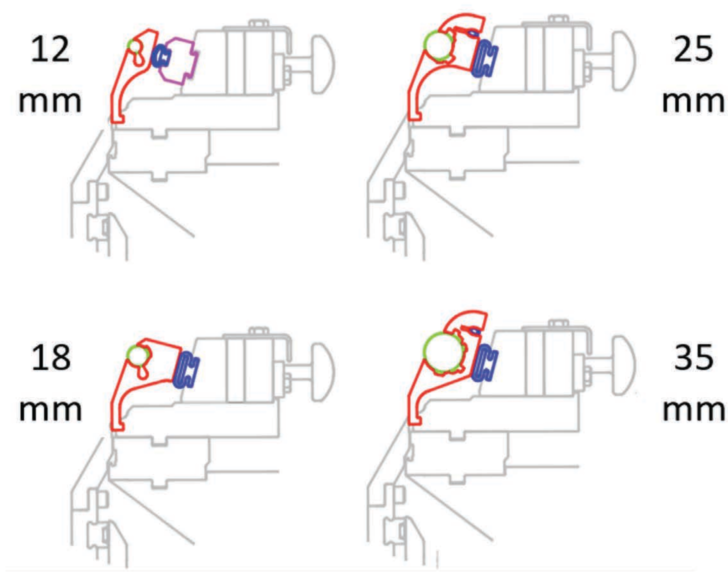

9. Schematic of rod holder geometries showing changes in how tube pressure is transmitted.

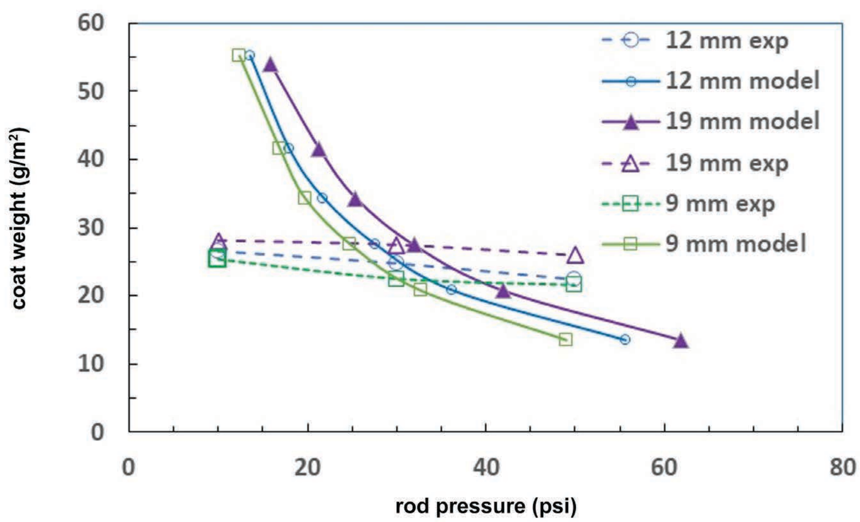

10. Comparison of coat weight response to rod pressure for three rod sizes for web velocity of 2.5 m/s and coating solids of 64.8% with a high shear viscosity of 76 cp.

suring the force that the rod pushes against a force measuring system. For the purposes here, a calibration constant is used to match the coat weight obtained for the 64.8% solids case at 30-psi rod load for the speed of 2.5 m/s for each rod size. The pressure is multiplied by the rod diameter to give a force per unit width. This value is found to be around a factor of 35, 40, and 45 times higher than the model predictions for rod sizes of 9, 12, and 19 mm, respectively. Therefore, these factors are used to adjust the model predictions to compare the trends of the results.

Figure 10 shows the comparison of the model with the pilot trials for the three rod sizes at solids of 64.8% and a velocity of 2.5 m/s. The wet thickness is converted to coat weight knowing the solids and also using the solids to calculate the effective density of the coating. As can be seen, the model predicts a steeper response of coat weight to rod pressure than is seen in the pilot coater data. A number of issues can cause this response, including the rubber tube deformation reducing the transmitted load at high pressures; motion of the rod normal to the web being inhibited from mechanical friction; or assumptions in the model, such as not including the backing roll deformation, filter cake formation, the exit region of the rod, or extensional viscosity effects.

This comparison shows the complexity of the system but gives some hope that a deeper understanding is pos-

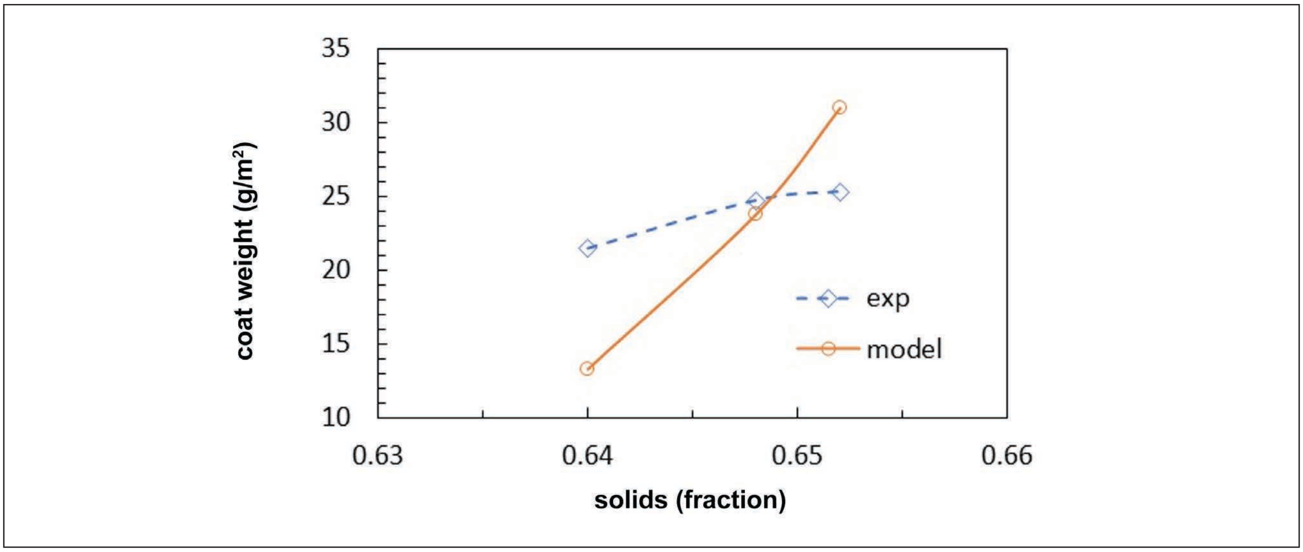

11. Comparison of the pilot trial with the model for rod diameter of 12 mm, speed of 2.5 m/s, and three solids levels at 30-psi rod load. The viscosities for 64, 64.8, and 65.2 solids are 61.4, 76.1, and 97.5 cps, respectively.

sible. As the rod load goes to zero, in theory, the coat weight should go to a high value as the model indicates, but the pilot data shows the coat weight going to some limit. As the tube pressure goes to a high value, the coat weight should decrease a significant amount. If this is not seen, the mechanism for the difference should give insight as to better control of this coating method.

The steepest response of the pilot coater data was the dependence of coat weight on solids. **Figure 11** compares the results for the 12-mm rod at 2.5 m/s at three solids. The model was run for various gaps until the pressure predictions matched the 30-psi load using the calibration factor. The model predicts that the dependence should be even steeper than what was seen in the trial. The high solids load has two effects: 1) the viscosity increases, and 2) the same wet thickness carries more solids. The increase in viscosity

ABOUT THE AUTHORS

Smooth rods are often used to apply barrier coatings, which have different rheology and lower solids than traditional paper coatings. This makes it difficult to select the proper combination of rod diameter, rod pressure, and coating rheology to get good control of coat weight. We felt that modeling could be a useful approach to predict these parameters. This research builds on our earlier work using modeling to understand the fundamentals of blade coater runnability.

The most difficult aspect of this research was validating the model predictions against experimental results. This was addressed by getting access to pilot coater run conditions for an earlier published study of smooth rod coatings on paperboard.

Personally, this research led to a deeper appreciation for the differences between blade and rod coating processes. The most surprising finding was the large impact of the shear thinning index on the coat weight vs. rod pressure response compared to the limited impact of high shear viscosity.

Mills might benefit from gaining the ability to get higher coat weights for low solids coatings by tuning the rheology profile of the coating to a desirable range shown in the model results. The next step in this research will be to incorporate additional features like filter cake formation into the model to better match with the experimental results.

Roper

Bousfield

Welsch

Roper is Fellow/consultant at PaperCote LLC in Midland, MI, USA. Bousfield is Calder professor in the Paper Surface Science program, Department of Chemical and Biomedical Engineering, at the University of Maine in Orono, ME, USA. Welsch is Global Innovation Leader for the Latex Binders Business at Trinseo LLC in Midland, MI, USA. Email Roper at jaroperiii@gmail.com.

causes a thicker wet layer to generate the same rod loading compared to a low viscosity coating.

Again, various assumptions of the model can explain the different trends. For example, if rubber deformation is taken into account, the shape of the nip changes, allowing less coating under the rod at the same rod loading. This would cause the high solids coat weight prediction to decrease and the low solids case to increase. More work is needed to understand why these trends are different.

CONCLUDING REMARKS

The influence of coating rheology on the coat weight control of a smooth rod is predicted using a finite element code neglecting other issues such as rubber deformation, cavitation, and film split phenomena. For the Newtonian cases, at low speeds and moderate viscosities, the coat weight-loading curve is steep, because there is not enough hydrodynamic lift at normal coat weight ranges to support rod loading. The Newtonian cases collapse onto a similar master curve for a wide range of parameters, whereas the Carreau model cases do not. By including shear thinning behavior, likely caused by a thickener addition, the coat weight/load curves are pushed to ranges that allow for good control of the coat weight. The correct values of parameters necessary to obtain this behavior will depend on the rod diameter, speed of operation, and the desired coat weight.

The coat weight vs. pressure response predicted by the model shows a much steeper change in coat weight as pressure is increased compared to pilot coater data. The reasons for this difference are not clear but could come from the differences in tube pressure-rod loading geometry or from neglecting fluid penetration and filter cake formation in the model. **TJ**

LITERATURE CITED

1. Reglat, O. and Tanguy, P., *TAPPI J.* 81(5): 195(1998).
2. Trefz, M. and Seiz, R., *TAPPI Metered Size Press Forum II, Proc.*, TAPPI Press, Atlanta, 1998, p. 85.
3. Kokko, A., Kuni, S., and Grankvist, T., *Adv. Coat. Fundam. Symp., Proc.*, TAPPI Press, Atlanta, 1999, p. 79.
4. Benjamin, D., Carvalho, M., and Anderson T., et al., *TAPPI Coating Conf., Proc.*, TAPPI Press, Atlanta, 1994, p. 109.
5. Carvalho, M. and Scriven, L., *TAPPI J.* 77(5): 201(1994).
6. Roper III, J. and Attal, J., *TAPPI J.* 76(5): 55(1993).
7. Pajari, H., Mansikka-aho, J., Ketoja, J., et al., *Adv. Coat. Fundam. Symp., Proc.*, TAPPI Press, Atlanta, 2003, p. 243.
8. Coyle, D.J., *Chem. Eng. Sci.* 43(10): 2673(1988). https://doi.org/10.1016/0009-2509(88)80011-3.
9. Hanumanthu, R. and Scriven, L., *Adv. Coat. Fundam. Symp., Proc.*, TAPPI Press, Atlanta, 1995, p. 109.
10. Alonso-Romero, S., "Metering film hydrodynamics in film coating," Ph.D. thesis, École Polytechnique Montreal, Montreal, 2000.
11. Cynecki, W., Welsch, G., Obermiller, D., et al., *Coat. Graphic Arts Conf.*, TAPPI Press, Atlanta, 2006, p. 155.

ABOUT THIS PAPER

Cite this article as:
Roper, J.A., III., Bousfield, D.W., and Welsch, G.W., *TAPPI J.* 21(11): 605(2022). https://doi.org/10.32964/TJ21.11.605

DOI: https://doi.org/10.32964/TJ21.11.605

ISSN: 0734-1415

Publisher: TAPPI Press

About this journal